Batteries & Supercaps

Research Article
doi.org/10.1002/batt.202500024

Chemistry Europe
European Chemical Societies Publishing

www.batteries-supercaps.org

Advanced Characterization of Lithium-Ion Battery Electrolytes Using Ultra-high Resolution Mass Spectrometry and Nuclear Magnetic Resonance Spectroscopy

Julien Maillard, Antonin Gajan, Charlotte Mase, Julien Demeaux, Olivier Serve, Sandra Mariette, Ludivine Afonso de Araujo, Hassan Oulyadi, Carlos Afonso,* and Pierre Giusti

Electricity storage is one of the key elements in the transition to renewable energy sources. Nowadays, the most common technology to meet this demand is the lithium-ion battery (LIB). The electrolytic solution composing these batteries is crucial for their good performance, as it determines the charging capacity and the lifetime through passivation processes. Among salts, additives and solvents that make up the electrolyte solution of LIBs, additional species can be present in a non-negligible amount. Such species may originate from impurities of added substances or from chemical reactions occurring during the operation of the batteries. All these components need to be characterized and quantified precisely to ensure good performances. However, electrolytic solutions are extremely sensitive to water and need to be manipulated under inert conditions. This constraint, together with their exotic molecular composition (numerous heteroatoms), increases the difficulty of the monitoring procedure. In the present work, we combine a molecular characterization and quantification approach using ultra-high resolution mass spectrometry and nuclear magnetic resonance to decipher a solution containing the most used electrolytes nowadays. The advantages and disadvantages of the used instruments are discussed.

1. Introduction

A key challenge for the success of the energy transition is the efficient storage of electrical energy. One of the keystone technology is the lithium-ion battery (LIB) which is the most widely used technology today.[1] Since its first commercialization in the 1990s, LIB has encountered numerous improvements but still requires enhancements to meet emerging challenges.[2] Nowadays, cocktails of non-aqueous electrolytes (composed of solvents, salts and additives) are used, and their composition differs depending on the electrode chemistries and desired application.[3] Among the electrolyte components, undesired species can be present in a non-negligible amount.[4] Such species can come, either from impurities of added substances in the cocktail or from chemical reactions occurring directly in the electrolyte solution.[5] Precise identification and quantification of all these electrolytic components is key to decipher the (electro)chemical reactions occurring within the system under operation. Several works are reported in the literature using gas chromatography,[6] ion chromatography,[7] inductively coupled plasma mass spectrometry (ICP-MS)[8] or nuclear magnetic resonance (NMR) to identify the degradation electrolyte degradation processes. High-resolution mass spectrometry (HRMS) has also recently allowed the characterization of the aging of $LiPF_6$-based LIB electrolytes.[9] However, in practice, the high heteroatomic diversity of electrolyte cocktails make this characterization challenging. One way to decipher the elemental complexity of electrolytes is by using ultra-high resolution mass spectrometry (UHRMS) such as Orbitrap and Fourier transform ion cyclotron resonance mass spectrometers (FTICR MS). These instrument, and especially FTICR MS, deliver the best performances in terms of mass accuracy, resolution, and dynamic ranges.[10] It allows the deep chemical characterization of highly

J. Maillard, C. Mase, O. Serve, S. Mariette, P. Giusti
TotalEnergies OneTech
TotalEnergies Research & Technology Gonfreville
BP 27, 76700 Harfleur, France

J. Maillard, C. Mase, C. Afonso, P. Giusti
International Joint Laboratory–iC2MC: Complex Matrices Molecular Characterization
TRTG, BP 27, 76700 Harfleur, France
E-mail: carlos.afonso@univ-rouen.fr

A. Gajan, J. Demeaux
Saft, Corporate Research
33074 Bordeaux, France

C. Mase, H. Oulyadi, C. Afonso, P. Giusti
Normandie Université, CARMeN, UMR 6064 et FR 3038
Université de Rouen, INSA de Rouen-Normandie, CNRS, IRCOF
76821 Mont-Saint-Aignan Cedex, France

L. Afonso de Araujo
TotalEnergies OneTech Belgium
B-7181 Seneffe, Belgium

Supporting information for this article is available on the WWW under https://doi.org/10.1002/batt.202500024

Research Article
doi.org/10.1002/batt.202500024
Chemistry Europe
European Chemical Societies Publishing

complex mixtures such as bio-oils, dissolved organic matter, or particulate matter.[11] Gas chromatography - Orbitrap MS was recently used to analyze the volatile fraction of electrolytes.[12] Characterization of the entire electrolyte is typically performed using electrospray-based direct infusion mass spectrometry, a selective ionization source that promotes the detection of acidic and basic compounds. Here, we propose a global characterization of electrolytes (volatiles and non-volatiles species) using FTICR MS coupled to a non-selective ionization source, atmospheric pressure chemical ionization (APCI).[13] Unlike ESI, APCI allows ionization of both polar and apolar species, primarily because ionization occurs in the gas phase in a nitrogen plasma. Because mass spectrometry cannot provide absolute quantification of species without standard molecules, nuclear magnetic resonance (NMR) spectroscopy was also used. For this purpose, a model electrolyte solution composed of components that are widely used in electrolytes was analyzed in positive and negative ion modes on an FTICR MS. The same solution was analyzed by NMR to identify signal of each component. Another fresh solution was used to quantify detected species. This work presents the first APCI-FTICR analysis of lithium-ion battery electrolytes that provides a comprehensive picture of the molecular content together with quantitative aspects thanks to NMR.

Table 1. List of components and their concentration in the S1, S2, S3 and S4 solutions. S1 corresponds to the solution with salts, additives, and solvents, S2 only the salts and additives and S3, S4 only the solvents and some additives.

Compound name	Acronym	S1 [g]	S2 [g]	S3 [g]	S4 [g]
Salts					
Lithium bis(fluorosulfonyl) imide	LiFSI	37.5	0.5	–	–
Lithium hexafluorophosphate	$LiPF_6$	121.5	0.5	–	–
Lithium difluoro(oxalate)borate	LiDFOB	3.2	0.5	–	–
Lithium bis(oxalate)borate	LiBOB	3.2	0.5	–	–
Additives					
Adiponitrile	ADN	1.6	–	0.1	–
Vinylcarbonate	VC	3.2	–	0.1	0.1
Fluoroethylene carbonate	FEC	3.2	0.5	0.1	–
Prop-1-ene-sultone	PES	1.6	0.5	0.1	–
1,3,2dioxathiolane-2,2-dioxide	DTD	1.6	0.5	0.1	–
Lithium difluorophosphate	LiDFP	1.6	0.5	–	–
Solvents					
Dimethyl carbonate	DMC	21.5	15.0	0.1	–
Methyl propionate	MP	18.3	–	0.1	–
Ethyl methyl carbonate	EMC	36.2	–	–	0.1
Ethyl carbonate	EC	10.6	–	–	0.1
Propylene carbonate	PC	19.3	–	–	0.1

2. Experimental Section

2.1. Electrolyte's Preparation

All the solvents, VC, FEC and $LiPF_6$ were provided by Soulbrain. ADN, DTD and PES were provided by Sigma Aldrich. LiBOB, LiDFOB, LiFSI were provided by Capchem. All the electrolytic solutions were prepared in argon-filled glovebox. **Table 1** presents the list of electrolytes and their concentration in the solutions S1–S4.

Structures of each are given in Figure S1, Supporting Information. Solution S1 includes all the salts, additives and solvents detailed above. Solution S2 includes only salts and additives while Solution S3 and S4 includes only solvents and some additives. The solutions S2, S3 and S4 have been prepared to set up the NMR quantification methods.

2.2. FTICR MS Analyses

2.2.1. Experiments

Solution S1 and solutions containing unique electrolytes components were used for the FTICR MS analysis. The solution S1 was diluted at 10^{-3} in DMC and the electrolytes were diluted at 10^{-6} in DMC. All the analyses were performed on a FTICR MS solariX XR from Bruker equipped with a 12 T superconducting magnet and APCI source. The mass spectrometer was externally calibrated with a solution of sodium trifluoroacetate. Mass spectra were afterwards internally calibrated with confidently assigned signals yielding a mass accuracy bellow 70 ppb in the considered mass range. Mass spectra were recorded in positive and negative ionization modes at 4 million points with a sum of 200 scans, yielding to a resolution of 500 000 at m/z 200. The following instrumental parameters were used: Capillary at 4500 V, Spray shield at −500 V, APCI temperature at 370 °C, Drying gas temperature at 220 °C, Corona needle at 5000 nA, Nebulizer gas flow at 1.5 bar, Injection flow rate 400 $\mu L\,h^{-1}$, Funnel 1 at −160 V, and Skimmer 1 at −15 V. Dimethyl carbonate (DMC) blank analysis was subtracted for each recorded spectrum to avoid external contaminants. Molecular formulas were obtained using the SmartFormula tool from DataAnalysis 5.3 software (Bruker).

2.2.2. Mass Defect Diagrams

In mass spectrometry, the mass defect is defined as the difference between the exact mass and the nominal mass.[14] As the mass defect depends on the molecular formula of the detected species, the mass defect versus nominal plots are very useful to describe data from complex mixtures within a bidimensional plot.[15] It should be pointed out that determination of the nominal mass requires knowledge of the molecular formula. Here, as it is generally done, the "nominal mass" was calculated by rounding the exact mass of the ion to the nearest integer. What is actually determined is therefore "apparent nominal mass" and "apparent mass defect" values (Equation (1)).[16]

$$\text{Mass defect} = \text{Exact mass} - \text{Nominal mass} \quad (1)$$

The mass defects of several elements composing lithium-ion batteries are given in **Figure 1**. As observed, hydrogen and boron have a positive mass defect whereas fluorine, phosphorus, and

Research Article
doi.org/10.1002/batt.202500024
Chemistry Europe
European Chemical Societies Publishing

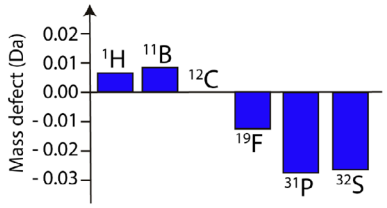

Figure 1. Mass defect of atoms encountered in the S1 solution.

sulfur have a negative one. Taking advantage of this molecular property, two-dimensional graphics were generated by representing the mass defect versus the nominal mass of all detected signals in each mass spectrum.

2.3. NMR Analyses

2.3.1. NMR Identification Experiments

NMR samples were prepared directly into a dry 5 mm NMR tube in an Argon glovebox to avoid sample degradation. The preparation consists in adding 200 µL of analyzed solutions to THF-d_8 (800 µL). The NMR (^{1}H, ^{13}C, ^{19}F, ^{31}P, ^{11}B) analyses of S1 mixture were performed on a Bruker Avance III 500 MHz spectrometer. Detailed information about the 1D and 2D experiments parameters can be found in the supporting information section.

2.3.2. Quantitative NMR (qNMR) Experiments

The optimization conditions and quantitative NMR measurements were performed on a Bruker Avance III 400 MHz. Measurements were obtained with internal standard methods and required the acquisition of spectra according to the following conditions: a relaxation delay equals to at least $5 \times T_1$, an acquisition time longer than $3 \times T_2$, and a signal to noise ratio at least 10:1. While it is straightforward to set up acquisition time and signal to noise, the measurement of T_1 requires a specific acquisition (all information in Supporting Information). Longitudinal relaxation times T_1 were measured with the inversion-recovery pulse sequence.[17] For ^{1}H and ^{11}B nuclei, the T_1 measurements were performed on a 10 mm BBO probe. Due to the inability of the BBO probe to measure ^{19}F, a 5 mm QNP probe was used.

3. Results and Discussion

3.1. FTICR MS Analyses

The S1 electrolyte (Table 1) was analyzed by APCI in the positive and negative ion modes. This ionization source allows the ionization of both polar and non-polar molecules, providing broad coverage of the chemical diversity of the molecules present in electrolytes. Resulting mass spectra are illustrated in **Figure 2**a for the positive ion mode and Figure 2b for the negative ion mode. The positive ion mode revealed a relatively simple mass spectrum with a total of 542 signals at signal-to-noise 5 between

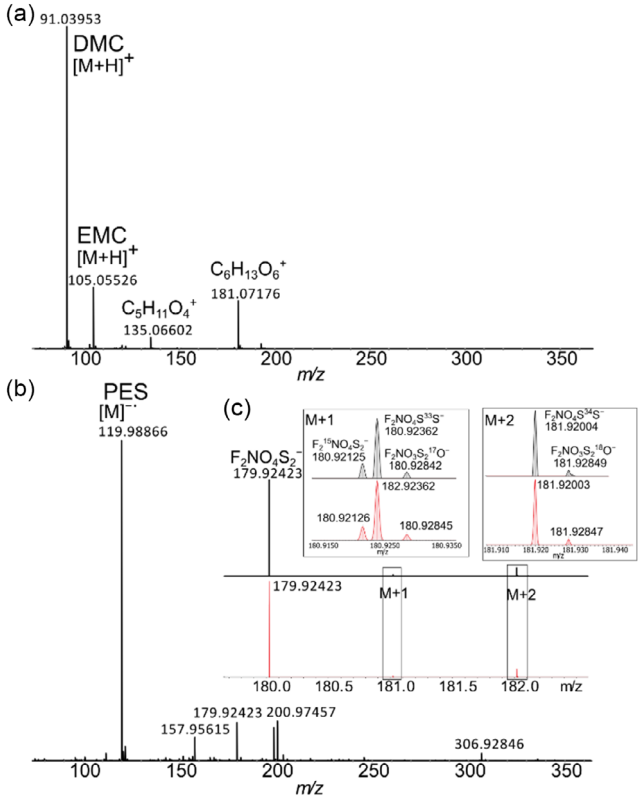

Figure 2. Obtained mass spectra of the S1 solution obtained in APCI in a) positive and b) negative ionization modes. The inset c) presents the attribution of the ion at m/z 179.92423 and the verification of its M + 1 and M + 2 isotopologues.

m/z 75 and m/z 400 corresponding to several solvents and their possible impurities. Intense species were attributed and reported on Figure 2a such as the DMC and the EMC detected as protonated molecules $[M + H]^{+}$. The DMC is the base peak, which was expected as it is the dilution solvent used to prepare the analyzed sample. In the same manner, the negative ion mode mass spectrum revealed ≈643 signals at signal-to-noise 5 ranging from m/z 75 to m/z 400. This mode allows the observation of the electrolyte salts and additives reported in the first part of Table 1. However, even with the relatively simple obtained spectrum, the molecular attribution was found to be very challenging. Indeed, salts and additives are composed of numerous heteroatoms such as boron, fluorine, phosphorus, and sulfur which increase drastically the amount of plausible molecular formula for one detected signal even with the extremely low mass deviation of 0.07 ppm in average obtained with the FTICR MS along the detected mass range. By taking advantage of the strong dynamic range, resolution and mass accuracy delivered by the mass spectrometer, it has been possible to validate several molecular formula attributions using the observation of their isotopologues. One example is given in Figure 2c. Here, the signal at m/z 179.92423 was attributed to the $F_2NO_4S_2^{-}$ molecular formula corresponding to LiFSI ($F_2NO_4S_2Li$) that lost the lithium cation. The simulated isotopic pattern of the molecular formula $F_2NO_4S_2^{-}$ was thus compared to the obtained mass spectrum and a perfect match between major isotopologues was found. However, this approach has two issues.

Research Article
doi.org/10.1002/batt.202500024
Chemistry Europe
European Chemical Societies Publishing

First, several heteroatoms such as the phosphorus and the fluorine have only one stable isotope and the isotopologues validation is thus, not possible. Then, this approach can only be applied to the most intense signals in order to detect low abundance isotopologues. Another methodology was thus required to have a global characterization of the S1 electrolyte.

As mentioned in the previous part, more than six hundred signals were detected in APCI(–)-FTICR MS at signal-to-noise 5. Molecular attribution and interpretation of the chemical pathway behind each species was then challenging. To simplify the puzzle, each salt and additive were analyzed individually in the same condition as the S1 solution. For each obtained mass spectrum, detected signals were extracted and represented according to their mass defect values versus nominal masses. The resulting two-dimensional map are given in **Figure 3**. Here, groups of points having the same color are from the same additive. It can be noticed that most of the species presents negative mass defect values except the boron-containing ones, which is consistent with values presented in Figure 1. Based on this representation, areas of existence were defined for each salt and additive, on the global view in Figure 3a and on the reduced range displayed by Figure 3b. In these areas, major species are signals coming from a particular additive. The attribution of species into each region is then easier because not all heteroatoms should be considered, which reduces drastically the amount of plausible molecular formula for one signal. In addition, it can allow a quick overview of species present in an electrolyte mixture. These defined regions were reported on the mass defect versus nominal mass of the whole S1 solution mass spectrum. The resulting map is given in Figure 3c,d. Molecular formulas that were confidently assigned are reported in Table S6, Supporting Information, for positive ion mode) and Table S7, Supporting Information, for negative ion mode.

3.2. NMR Analyses

In addition to the mass spectrometry analysis, we were interested in undertaking an NMR study to tackle quantitative measurements. The integral of the NMR signal resonating at a given frequency is directly related to the number of nuclei resonating at that frequency, endowing NMR with inherent quantitative capabilities suitable for analytical applications. The S1 solution bearing six magnetically active nuclei (^{1}H, ^{7}Li, ^{13}C, ^{11}B, ^{19}F and ^{31}P), is therefore particularly well-suited for NMR analysis. This allows for the simultaneous observation of the NMR-active nuclei, providing an in situ picture of the species present in the mixture and their relative proportions. However, in the case of complex mixtures, high spectral resolution and accurate signal assignment on NMR

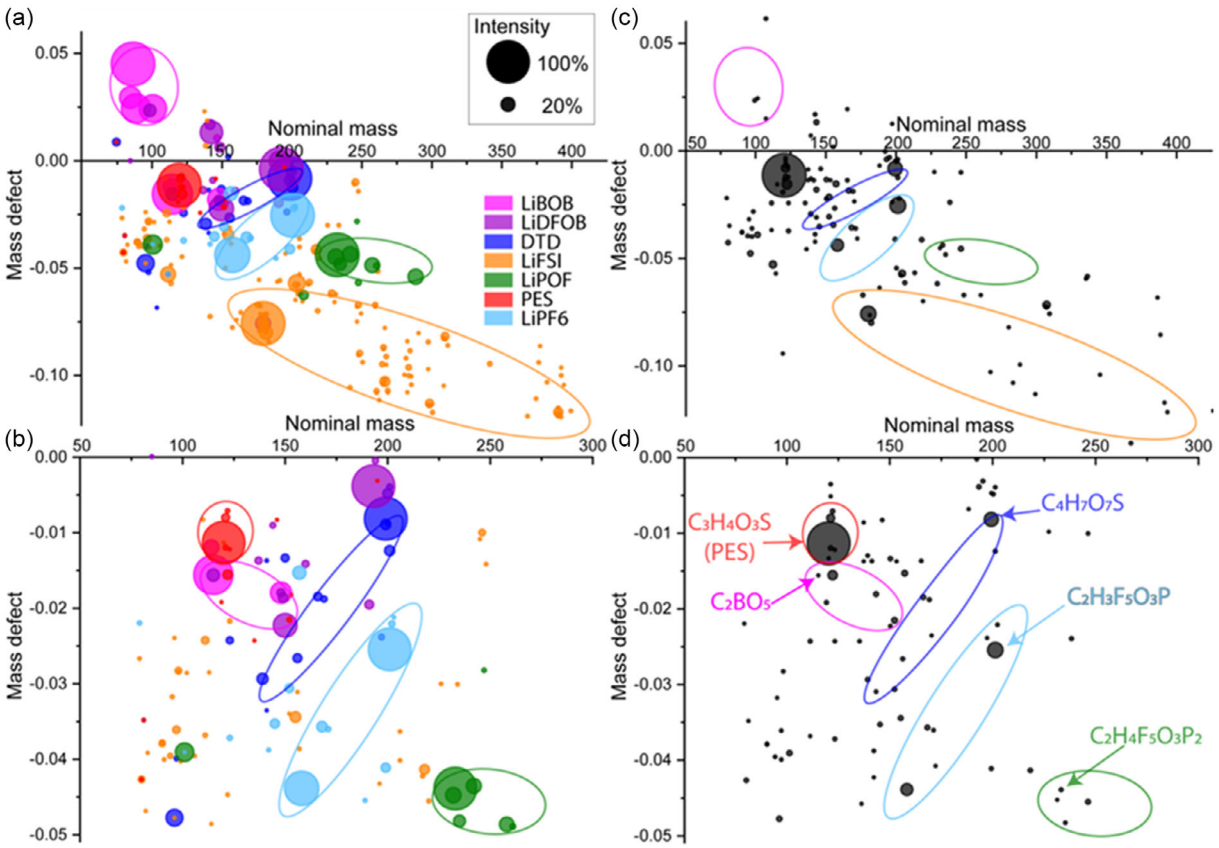

Figure 3. (in left) Mass defect versus nominal mass representation of all ions detected for each electrolyte salt and additive analyzed individually. a) Full range, b) zoom. Signals coming from the same salt and additive mass spectrum have the same color. The size of dots represents the intensity of the signal in the mass spectrum. The intensity of each set of signals were normalized from 0 to 100 for each additive. (in right) Mass defect versus nominal mass representation of all ions detected for the S1 solution. c) Full range, d) zoom. The size of dots represents the intensity of the signal in the mass spectrum. The intensity of each set of signals were normalized from 0 to 100.

Research Article
doi.org/10.1002/batt.202500024
Chemistry Europe
European Chemical Societies Publishing

spectra is a prerequisite for quantitative measurements. To do this, the S1 solution was prepared in THF-d_8 and then a (^{1}H, ^{7}Li, ^{11}B, ^{13}C, ^{19}F, ^{31}P) multinuclear NMR analysis was carried out.

3.2.1. Identification

The ^{1}H NMR spectrum given in **Figure 4** shows a high enough signal resolution to allow, thanks to the two-dimensional NMR experiments ^{1}H/^{1}H COSY (Figure S1, Supporting Information), the ^{1}H/^{13}C HMQC and HMBC (Figure S2 and S3, Supporting Information), an assignment of the signals to each component of the S1 solution. All ^{1}H and ^{13}C chemical shifts of the organic solvents and additives are summarized in Table S2, Supporting Information.

The nuclei present in the salt and additive species are ideal for characterization by NMR spectroscopy. The ^{19}F and ^{31}P exhibit high and mid gyromagnetic ratios, respectively, and both are spin ½ nuclei with a natural abundance of 100%. While the isotopes ^{7}Li and ^{11}B exhibit mid gyromagnetic ratios, and both are spin 3/2 with a natural abundance of 92.58% and 80.42% respectively.

The ^{31}P spectrum of the S1 solution showed two major signals characteristic of the ^{31}P atoms of $LiPF_6$ and LiDFP (**Figure 5**). The signal at −144.3 ppm shows a septet with $^1J_{P\text{-}F} = 707$ Hz. It has been attributed to $LiPF_6$. The signal at −19.3 ppm shows a triplet, $^1J_{P\text{-}F} = 927$ Hz, and was therefore attributed to LiDFP.

In the ^{19}F spectrum (Figure 5), the fluorinated signals of $LiPF_6$ and LiDFP are easily identifiable by their doublet multiplicity and scalar coupling values. The doublet signals at −74.9 ppm, $^1J_{P\text{-}F} = 707$ Hz and at −85 ppm, $^1J_{P\text{-}F} = 927$ Hz, were assigned to LiPF6 and LiDFP respectively. In addition, the ^{19}F NMR spectrum contains a singlet at 51.2 ppm corresponding to the two fluorine atoms of LiFSI, two signals, at −155.37 and −156.87 ppm, corresponding to the two fluorine atoms of LiDFOB and a multiplet, that simplifies to a singlet on the fluorine decoupled proton spectrum, assigned to FEC (−158.8 ppm) (**Figure 6**).

To get more information about the Boron containing electrolytes, ^{11}B NMR spectroscopy was applied. The spectrum shows the two major signals at 7.9 and 3.0 ppm corresponding respectively to LiDFOB and LiBOB.

It is noteworthy that minor signals are observed in the ^{31}P, ^{19}F and ^{11}B spectra. These signals are probably due to the degradation of the electrolytes (possible partial decomposition of the Li salt by hydrolysis upon storage) (**Figure 7**).

3.2.2. Quantitative NMR Measurements

The quantification procedure is detailed in the Methods & Materials part. To develop this method, several solutions (S2, S3 and S4) were prepared where the proportion of each component is precisely known. Identification of signals was also performed and is reported by Figure S4, Supporting Information, to S6. Relaxation times T1 were measured for each nuclei (See Supporting information) and relaxation delay equals to at least 5 × T1 were used to acquire quantitative (^{1}H, ^{11}B, ^{19}F and ^{31}P) qNMR spectra and quantify each components of these solutions.

^{1}H and ^{19}F qNMR analyses lead to the results presented in the **Table 2** for S2, S3 and S4 whose composition is known (%m calc). Thanks to calculations we obtained the mass percentages based on NMR spectra (%m NMR).

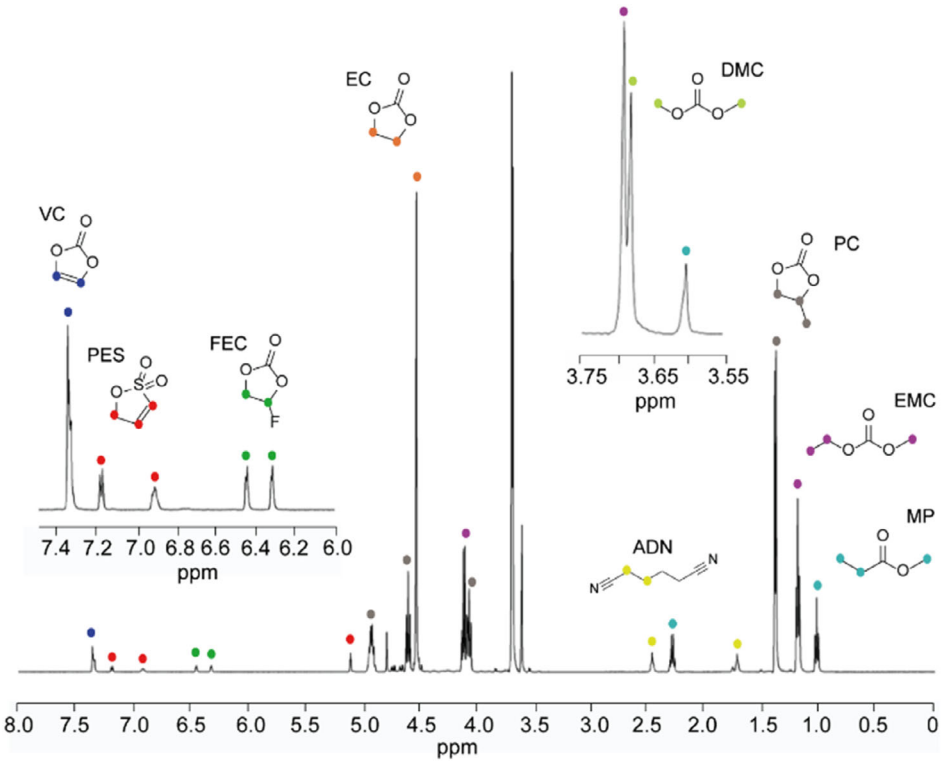

Figure 4. 1D ^{1}H spectrum (500 MHz) of S1 in THF-d8 at 298 K.

Research Article
doi.org/10.1002/batt.202500024
Chemistry Europe
European Chemical Societies Publishing

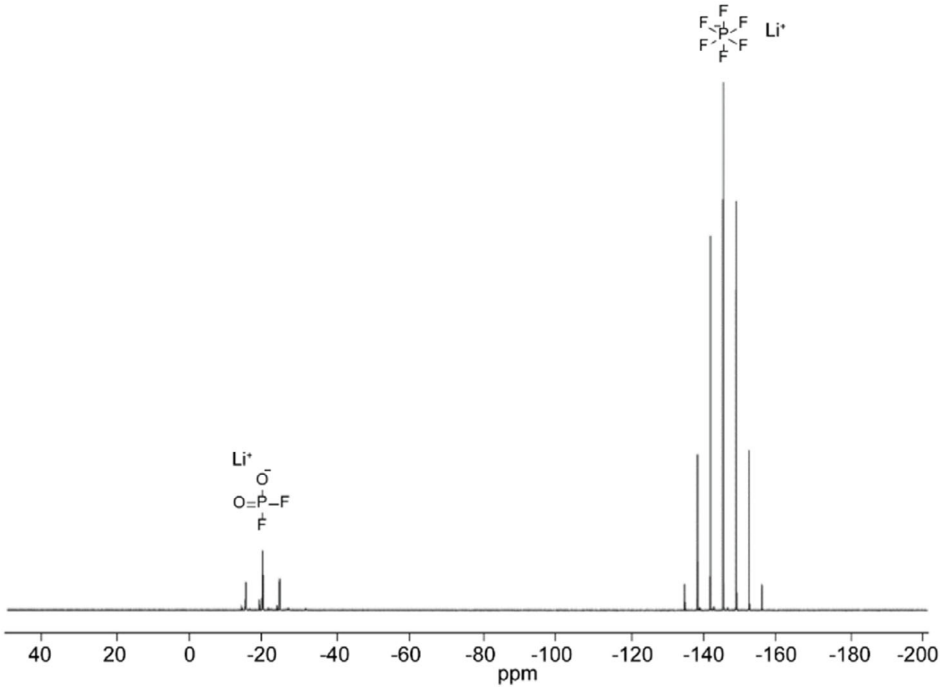

Figure 5. 1D 31 P spectrum (202 MHz) of S1 solution in THF-d_8 at 298 K.

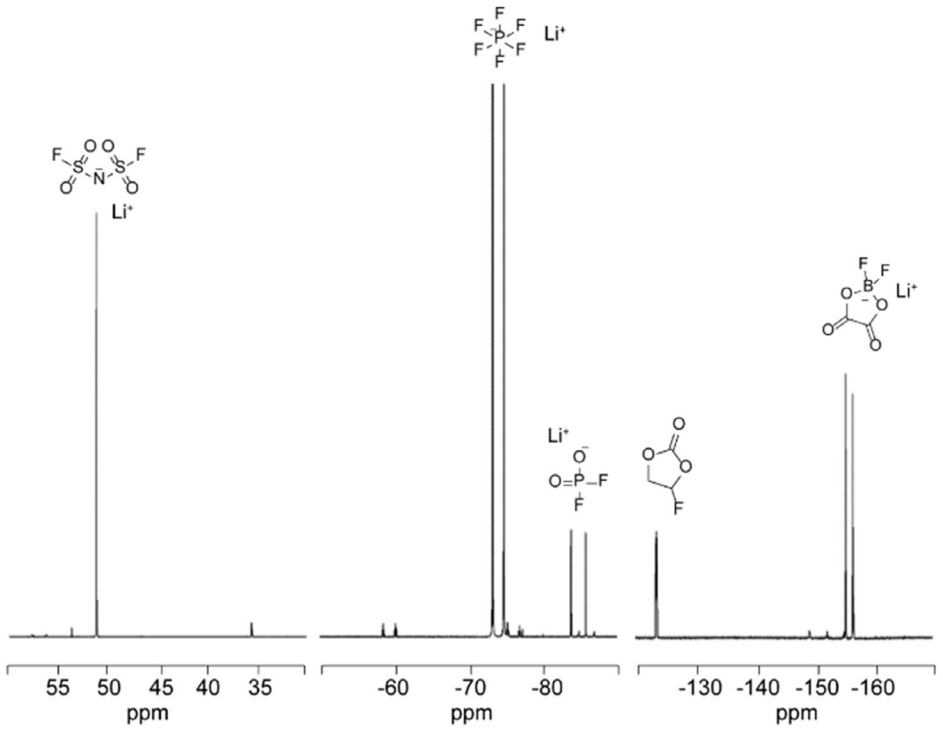

Figure 6. 1D ^{19}F spectrum (470 MHz) of S1 in THF-d8 at 298 K.

The FEC component has both ^{1}H and ^{19}F nuclei, we can then compare the NMR quantitative methods on both nuclei. By ^{1}H NMR, we obtained 2.81% and by ^{19}F NMR we obtained 2.75%. Those values present an average deviation of 0.28% compared to real values, confirming the robustness of the quantitative methods by ^{1}H and ^{19}F NMR. For the quantification, we chose to maintain the value obtained by ^{19}F NMR because the FEC peak is well resolved, washing any doubts about overlapping issues due to the bigger chemical shifts range than ^{1}H NMR spectrum.

We observe a discrepancy of 3.40% in the total quantification. Of this figure, 2.62% can be attributed to undermined LiBOB, leaving ≈0.78% of unknown components. This discrepancy of 0.78%

Research Article
doi.org/10.1002/batt.202500024
Chemistry Europe
European Chemical Societies Publishing

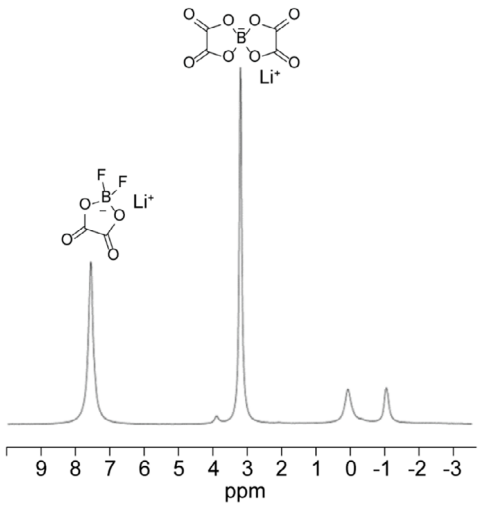

Figure 7. 1D ^{11}B spectrum (160 MHz) of S1 solution in THF-d_8 at 298 K.

Table 2. Results of the quantification of the sol. 2, 3 and 4 using NMR.

Solution S2	Solution S3	Solution S4	Weighted mass [g]	%m calc	%m NMR
LiFSI	–	–	0.498	2.61%	2.40%
LiPF6	–	–	0.501	2.63%	2.48%
LiDFP	–	–	0.497	2.61%	2.49%
LiDFOB	–	–	0.506	2.65%	2.81%
PES	–	–	0.509	2.67%	2.71%
DTD	–	–	0.498	2.61%	2.05%
LiBOB	–	–	0.499	2.62%	n/d
FEC	–	–	0.527	2.76%	2.75%
DMC	–	–	15.027	78.83%	78.92%
TOTAL	–	–	19.062	100%	96.60%
–	VC	–	0.1294	15.15%	14.91%
–	FEC	–	0.1146	13.41%	12.97%
–	PES	–	0.1131	13.24%	13.26%
–	DTD	–	0.116	13.58%	12.47%
–	MP	–	0.1388	16.25%	16.70%
–	ADN	–	0.1187	13.89%	13.86%
–	DMC	–	0.1238	14.49%	13.88%
–	TOTAL	–	0.8544	100.00%	98.05%
–	–	VC	0.0944	21.21%	21.36%
–	–	PC	0.1037	23.30%	24.53%
–	–	EC	0.1238	27.81%	25.55%
–	–	EMC	0.1232	27.68%	27.70%
–	–	TOTAL	0.4451	100.0%	99.13%

may be explained by a slight integration error of the signals, resulting in a systematic error in the calculated percentage for each compound. It could also arise from minor degradation of compounds, which could lead to the formation of other species not accounted for in the percentage calculations. Indeed, low-intensity signals, characteristic of unidentified species, are clearly visible in the ^{1}H, ^{31}P, and ^{19}F spectra (Figure S4–S6, Supporting Information).

4. Discussion

Main challenges of the characterization of LIB materials are the identification and the quantification. In this regard, powerful analytical methods have been used and each was rather suitable for the identification or the quantification. FTICR MS and NMR allowed the precise identification and quantification of the components of the S1 electrolyte, which includes all solvents, salts and additives chosen in the frame of this study. FTICR MS allowed the identification of most of the constituents of the solution S1 in one analysis of few minutes. Hundreds of additional species corresponding to some impurities were also evidenced. These contaminants are of particular interest because of their potential impact on the battery performance. Bi-dimensional mass defect *versus* nominal mass graphs have demonstrated the ability to quickly recognize the constituent of electrolytes mixtures even without molecular attribution and thus, it can be used on more routinely usable instruments. To speed up the identification of future electrolytes mixture, such patterns can be saved and used directly using a script. Results obtained in FTICR MS have shown its ability to detect the presence of all additives but not all solvents. They were either in too small amount compared to the dilution solvent (DMC) or have a mass too small to be detected by the instrument ($<$m/z 75).

FTICR MS affords only limited quantitative information as signal intensity is related to a specific response factor that is unknown without the use of proper calibration procedure with standard molecules. In the other hand, NMR allowed the quantification of components of S2, S3 and S4 solutions. To achieve this, five specific nuclei (^{1}H, ^{13}C, ^{11}B, ^{19}F, and ^{31}P) were selected, and several 1D and 2D NMR experiments were conducted and analyzed. This provided a precise in situ picture of the species present in each mixture and allowed for the determination of their relative proportions. The ^{1}H and ^{19}F qNMR allowed for the quantification of all components with high accuracy, except for LiBOB. The quantification of this compound can only be obtained from a ^{11}B NMR spectrum. Unfortunately, despite testing various internal standard candidates for the ^{11}B qNMR experiments, we did not find a standard compatible with our Li-ion electrolyte solutions.

5. Conclusion

In this work, the complementarity between NMR and FTICR MS was observed for the characterization of Lithium-ion battery electrolytes. The sub-ppm mass accuracy of the FTICR MS has allowed the molecular assignments of detected species. By taking advantage of the isotopic fine structure, even species with high heteroatomic content (phosphorus, fluorine, boron, sulfur) were identified with confidence, allowing a new overview of the chemical dispersity in such electrolytic solution. Fingerprints of the sample were generated using mass defect versus nominal mass cartographies. This new approach has highlighted the hidden composition of the analyzed cocktail and will be useful for the understanding of chemical processes occurring in lithium-ion batteries. In addition, it can be applied for the monitoring of

ageing process or the quality control of purchased electrolytic solutions. In the meantime, the quantification of electrolytes components was developed using NMR. The disadvantages and advantages of each technique were discussed.

Supporting Information

Detailed experimental procedures, analytical data, NMR spectra, and HPLC traces are provided in the Supporting Information. Additional references cited within the Supporting Information.[17–41]

Acknowledgements

This work has been partially supported by Universityof Rouen Normandy, INSA Rouen Normandy, the Centre National de la Recherche Scientifique (CNRS), European Regional Development Fund (ERDF), Labex SynOrg (ANR-11-LABX-0029), Carnot Institute I2C, the graduate school for research XL-Chem (ANR-18-EURE-0020 XL CHEM), Region Normandie. Access to the CNRS research-infrastructure Infranalytics (FR2054) is gratefully acknowledged.

Conflict of Interest

The authors declare no conflict of interest.

Data Availability Statement

The data that support the findings of this study are available in the supplementary material of this article.

Keywords: characterization · electrolyte · mass spectrometry · nuclear magnetic resonance

[1] M. S. Dresselhaus, I. L. Thomas, *Nature* **2001**, *414*, 332.
[2] a) M. Winter, B. Barnett, K. Xu, *Chem. Rev.* **2018**, *118*, 11433; b) G. E. Blomgren, *J. Electrochem. Soc.* **2017**, *164*, A5019; c) M. Armand, P. Axmann, D. Bresser, M. Copley, K. Edström, C. Ekberg, D. Guyomard, B. Lestriez, P. Novák, M. Petranikova, W. Porcher, S. Trabesinger, M. Wohlfahrt-Mehrens, H. Zhang, *J. Power Sources* **2020**, *479*, 228708; d) F. Schipper, D. Aurbach, *Russ. J. Electrochem.* **2016**, *52*, 1095; e) T. Placke, R. Kloepsch, S. Dühnen, M. Winter, *J. Solid State Electrochem.* **2017**, *21*, 1939.
[3] a) J.-G. Zhang, W. Xu, J. Xiao, X. Cao, J. Liu, *Chem. Rev.* **2020**, *120*, 13312; b) H. Jia, W. Xu, *Curr. Opin. Electrochem.* **2021**, *30*, 100781; c) K. Xu, *Chem. Rev.* **2004**, *104*, 4303; d) S. Tan, Y. J. Ji, Z. R. Zhang, Y. Yang, *ChemPhysChem* **2014**, *15*, 1956; e) M. Ue, Y. Sasaki, Y. Tanaka, M. Morita, *Electrolytes for Lithium and Lithium-Ion Batteries* (Eds: T. R. Jow, K. Xu, O. Borodin, M. Ue), Springer New York, New York, NY **2014**, pp. 93–165; f) W. A. Henderson, *Electrolytes for Lithium and Lithium-Ion Batteries* (Eds: T. R. Jow, K. Xu, O. Borodin, M. Ue), Springer New York, New York, NY **2014**, pp. 1–92; g) K. Abe, *Electrolytes for Lithium and Lithium-Ion Batteries* (Eds: T. R. Jow, K. Xu, O. Borodin, M. Ue), Springer New York, New York, NY **2014**, pp. 167–207.
[4] a) L. Yang, M. M. Furczon, A. Xiao, B. L. Lucht, Z. Zhang, D. P. Abraham, *J. Power Sources* **2010**, *195*, 1698; b) U. Heider, R. Oesten, M. Jungnitz, *J. Power Sources* **1999**, *81–82*, 119; c) P. Handel, G. Fauler, K. Kapper, M. Schmuck, C. Stangl, R. Fischer, F. Uhlig, S. Koller, *J. Power Sources* **2014**, *267*, 255.
[5] H. Matsumoto, *Electrolytes For Lithium And Lithium-Ion Batteries* (Eds: T. R. Jow, K. Xu, O. Borodin, M. Ue), Springer New York, New York, NY **2014**, pp. 209–225.
[6] F. Horsthemke, A. Friesen, X. Mönnighoff, Y. P. Stenzel, M. Grützke, J. T. Andersson, M. Winter, S. Nowak, *RSC Adv.* **2017**, *7*, 46989.
[7] W. Weber, R. Wagner, B. Streipert, V. Kraft, M. Winter, S. Nowak, *J. Power Sources* **2016**, *306*, 193.
[8] a) L. Fu, H. Xie, J. Huang, X. Chen, L. Chen, *Spectrochim. Acta Part B: At. Spectrosc.* **2021**, *181*, 106217; b) B. L. D. Rinkel, D. S. Hall, I. Temprano, C. P. Grey, *J. Am. Chem. Soc.* **2020**, *142*, 15058; c) J. Henschel, C. Peschel, S. Klein, F. Horsthemke, M. Winter, S. Nowak, *Angew. Chem. Int. Ed.* **2020**, *59*, 6128.
[9] a) S. Wiemers-Meyer, M. Winter, S. Nowak, *Phys. Chem. Chem. Phys.* **2016**, *18*, 26595; b) K. Kösters, J. Henschel, M. Winter, S. Nowak, *J. Chromatogr. A* **2021**, *1624*, 462594; c) S. Takeda, W. Morimura, Y.-H. Liu, T. Sakai, Y. Saito, *Rapid Commun. Mass Spectrom.* **2016**, *30*, 1754; d) B. Vortmann, S. Nowak, C. Engelhard, *Anal. Chem.* **2013**, *85*, 3433; e) G. Gachot, P. Ribiere, D. Mathiron, S. Grugeon, M. Armand, J. B. Leriche, S. Pilard, S. Laruelle, *Anal. Chem.* **2011**, *83*, 478.
[10] D. F. Smith, D. C. Podgorski, R. P. Rodgers, G. T. Blakney, C. L. Hendrickson, *Anal. Chem.* **2018**, *90*, 2041.
[11] W. Bahureksa, T. Borch, R. B. Young, C. R. Weisbrod, G. T. Blakney, A. M. McKenna, *Anal. Chem.* **2022**, *94*, 11382.
[12] C. Peschel, F. Horsthemke, M. Winter, S. Nowak, *MethodsX* **2022**, *9*, 101621.
[13] C. Mase, M. Hubert-Roux, C. Afonso, P. Giusti, *J. Anal. Appl. Pyrolysis* **2022**, *167*, 105694.
[14] L. Sleno, *J. Mass Spectrom.* **2012**, *47*, 226.
[15] C. Wolters, V. Vuitton, F.-R. Orthous-Daunay, L. Flandinet, C. He, S. E. Moran, S. M. Hörst, *ACS Earth Space Chem.* **2023**.
[16] O. Lacroix-Andrivet, S. Moualdi, M. Hubert-Roux, C. Loutelier Bourhis, A. L. Mendes Siqueira, C. Afonso, *J. Am. Soc. Mass Spectrom.* **2022**, *33*, 1194.
[17] E. L. Hahn, *Physical Review* **1949**, *76*, 145.

Manuscript received: January 13, 2025
Revised manuscript received: March 7, 2025
Version of record online: March 31, 2025